



AR-C155858 is a potent inhibitor of monocarboxylate transporters MCT1 and MCT2 that binds to an intracellular site involving transmembrane helices 7–10

Matthew J. OVENS*, Andrew J. DAVIES*, Marieangela C. WILSON*, Clare M. MURRAY† and Andrew P. HALESTRAP*¹

*Department of Biochemistry, School of Medical Sciences, University of Bristol, University Walk, Bristol BS8 1TD, U.K., and †Bioscience Department, AstraZeneca R&D Charnwood, Bakewell Road, Loughborough, Leicestershire LE11 5RH, U.K.

In the present study we characterize the properties of the potent MCT1 (monocarboxylate transporter 1) inhibitor AR-C155858. Inhibitor titrations of L-lactate transport by MCT1 in rat erythrocytes were used to determine the K_i value and number of AR-C155858-binding sites (Et) on MCT1 and the turnover number of the transporter (k_{cat}). Derived values were 2.3 ± 1.4 nM, 1.29 ± 0.09 nmol per ml of packed cells and 12.2 ± 1.1 s⁻¹ respectively. When expressed in *Xenopus laevis* oocytes, MCT1 and MCT2 were potently inhibited by AR-C155858, whereas MCT4 was not. Inhibition of MCT1 was shown to be time-dependent, and the compound was also active when microinjected, suggesting that AR-C155858 probably enters the cell before binding to an intracellular site on MCT1. Measurement of the inhibitor sensitivity of several chimaeric transporters combining different domains of MCT1 and MCT4 revealed that the binding

site for AR-C155858 is contained within the C-terminal half of MCT1, and involves TM (transmembrane) domains 7–10. This is consistent with previous data identifying Phe³⁶⁰ (in TM10) and Asp³⁰² plus Arg³⁰⁶ (TM8) as key residues in substrate binding and translocation by MCT1. Measurement of the K_m values of the chimaeras for L-lactate and pyruvate demonstrate that both the C- and N-terminal halves of the molecule influence transport kinetics consistent with our proposed molecular model of MCT1 and its translocation mechanism that requires Lys³⁸ in TM1 in addition to Asp³⁰² and Arg³⁰⁶ in TM8 [Wilson, Meredith, Bunnun, Sessions and Halestrap (2009) J. Biol. Chem. **284**, 20011–20021].

Key words: chimaeric transporter, erythrocyte, lactate transport, monocarboxylate transporter (MCT), *Xenopus* oocytes.

INTRODUCTION

There are 14 members of the MCT (monocarboxylate transporter) family (SLC16) encoded by the human and mouse genomes [1]. Of these only MCT1, MCT2, MCT3 and MCT4 have been demonstrated to catalyse the bidirectional proton-linked transport of short-chain monocarboxylates such as L-lactate and pyruvate across the plasma membrane of mammalian cells [2–6]. MCT1 is expressed in most tissues and facilitates lactic acid uptake for oxidation in heart and red skeletal muscle, and for gluconeogenesis in the liver and kidney of some species [7–11]. MCT1 is also used for lactic acid efflux by some cells that are exclusively glycolytic, such as erythrocytes, and by all cells under hypoxic conditions [1,10,12]. MCT2 is a higher-affinity transporter [3] whose expression is more restricted and highly species-dependent [1]. In some species it is the dominant MCT isoform in the kidney and liver where it facilitates lactic acid uptake for gluconeogenesis [9,13]. It is also expressed in neurons, especially at the post-synaptic density, and has been proposed to provide the uptake pathway for the oxidation of lactate produced by the more glycolytic astrocytes [14,15]. MCT3 expression is confined to the basal membrane of the retinal pigment epithelium and choroid plexus epithelia [16,17], but detailed information on its substrate and inhibitor specificity is lacking [4]. MCT4 is a lower-affinity transporter [5,6] and is primarily expressed in highly glycolytic cells, such as white muscle fibres, where it is used to facilitate lactic acid efflux from the tissue [18,19]. Most cells can up-regulate MCT4 expression under hypoxic conditions

when glycolytic flux is enhanced and this is mediated through transcriptional control by HIF-1 α (hypoxia-inducible factor 1 α) [20].

In view of the importance of plasma membrane lactic acid transport in metabolism, it would be desirable to have a specific inhibitor of each isoform that could probe their individual metabolic roles. A range of inhibitors of MCTs have been described, including the α -cyanocinnamate derivatives, stilbene disulfonates such as DIDS (di-isothiocyanostilbene disulfonate), phloretin, bioflavonoids such as quercetin and organomercurial reagents such as p-chlomercuribenzene sulfonate (see [1,21,22]). However, none of these is specific for inhibition of MCTs and thus they cannot be used with confidence in metabolic studies. This reservation applies particularly to α -cyano-4-hydroxycinnamate that some workers have used on the assumption that it is a specific MCT inhibitor (for example see [23–25]). However, this agent is at least two orders of magnitude more potent at inhibiting the mitochondrial pyruvate carrier than MCT1 [26–29]. Previously, a new class of specific and extremely high-affinity inhibitors of MCT1 have been discovered by AstraZeneca [30–32]. These compounds were originally identified as potent inhibitors of T-lymphocyte proliferation that act as immunosuppressants and were subsequently shown to bind to MCT1 and MCT2, but not MCT4 [30]. Since T-lymphocyte activation and proliferation is accompanied by a large (up to 14-fold) stimulation of glycolysis, it would appear that inhibiting MCT1 and so preventing the efflux of the resulting lactic acid is responsible for the compounds' immunosuppressive activity [30].

Abbreviations used: BCECF, 2'-7'-bis(carboxyethyl)-5(6)-carboxyfluorescein; DIDS, di-isothiocyanostilbene disulfonate; MCT, monocarboxylate transporter; TM, transmembrane.

¹ To whom correspondence should be addressed (email a.halestrap@bristol.ac.uk).

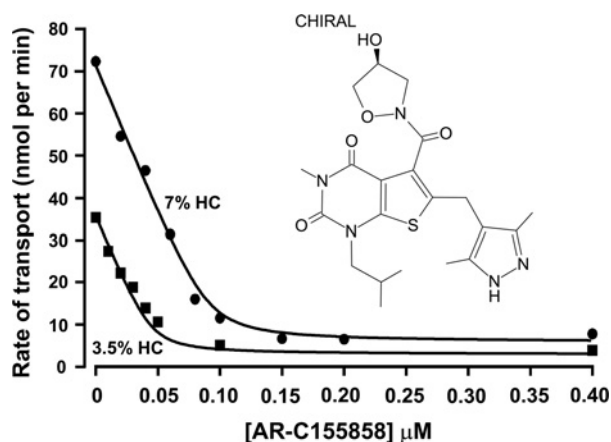


Figure 1 Inhibition of L-lactate uptake into rat erythrocytes by AR-C155858

Rat erythrocytes were freshly isolated and resuspended at the specified haematocrit as outlined in the Experimental section. Cells were pre-incubated for 1 h at room temperature in the presence or absence of the specified concentration of AR-C155858 (structure shown). Transport was measured by continuous monitoring of the extracellular pH, and calibration of pH changes in terms of proton uptake was achieved by addition of standardized NaOH (10 μ M final) just before addition of 10 mM L-lactate to initiate transport. Initial rates of transport were calculated by first-order regression analysis of the time course of pH change. The data were then fitted by non-linear least squares inhibition to the equation for a tight-binding non-competitive inhibitor using inhibitor concentration and haematocrit as the two x -variables [41,42]. The derived values (\pm S.E. of the fit shown) for the K_i and concentration of binding sites were 2.3 ± 1.4 nM and 1.29 ± 0.09 nmol per ml of packed cells respectively.

In the present study we seek to characterize the mode of action of one of these potent MCT1 inhibitors, AR-C155858. We have studied the concentration dependency of AR-C155858 inhibition of lactate transport into rat erythrocytes mediated by endogenous MCT1, as well as its effects on the activity of MCT1, MCT2 and MCT4 expressed in *Xenopus laevis* oocytes. We show that AR-C155858 inhibits MCT1 and MCT2 with similar potency, but is inactive against MCT4, and that inhibition is exerted by the drug binding to a site on MCT1 accessible from the cytosol. The use of MCT1/MCT4 chimaeric transporters reveals that this binding site is contained within TM (transmembrane) helices 7–10 of MCT1. In rat erythrocytes a detailed analysis of the inhibition of lactate transport by AR-C155858 has enabled us to determine the turnover number (k_{cat}) of MCT1 (12.2 s^{-1} at 6°C) and the K_i value for AR-C155858 (2.3 nM).

EXPERIMENTAL

Materials

X. laevis toads were obtained from Xenopus Express and oocytes were harvested as described previously [33]. All reagents were obtained from Sigma unless otherwise stated. Polyclonal antibodies against the C-terminal 16 amino acids of rat MCT1, MCT2 and MCT4, and against a 17 amino acid sequence between TM7 and TM8 of MCT1 were raised in rabbits as described previously [9,18,34]. Anti-rabbit secondary antibodies for immunofluorescence microscopy were from Jackson ImmunoResearch. L-[14 C]Lactate was obtained from GE Healthcare and [14 C]pyruvate was from PerkinElmer. AR-C155858 (whose structure is shown as an inset to Figure 1) was obtained from AstraZeneca and made up as a 10 mM stock in DMSO.

Methods

Generation of MCT chimaeras of rat MCT1 and MCT4 was performed by PCR using pfu Taq polymerase (Roche). The two appropriate segments of MCT1 and MCT4 were produced with a region of overlapping sequence that was used to splice the two together to produce the desired chimaera. For the MCT1/4 and MCT4/1 chimaeras the switch occurs at the end of the loop between TMs 6 and 7 which contains the conserved sequence LDLS. For the MCT1/4TM11 and MCT4/1TM11 chimaera the switch occurs at the beginning of TM11 containing the conserved sequence FSSA. However, for the C-terminal chimaeras MCT1/4c and MCT4/1c, where the switch occurs at the beginning of the C-terminus, there is no conserved sequence and thus a region of complementarity was manufactured using modified primers [35]. A C-terminal truncation of MCT1 was produced using PCR to amplify the MCT1 sequence minus the C-terminus, and this was subsequently inserted into the oocyte expression vector pGHJ with the addition of a stop codon in the vector downstream of the MCT sequence. Sequences for all primers used are given in Supplementary Table S1 (at <http://www.BiochemJ.org/bj/425/bj4250523add.htm>) and were designed to be between 15 and 30 bases in length. Typically, for an MCT fragment, thermocycling was performed using the following parameters: 30 s at 95°C, 30 s at 55°C and a 1.5 min extension at 72°C for 30 cycles. Subsequently, appropriate fragments of MCT1 and MCT4 with complementary sequence in the crossover region were combined using PCR with primers to the 5'- and 3'-UTR (untranslated region) of MCT1 and MCT4. Here, thermocycling was performed using the following parameters: 30 s at 95°C, 30 s at 55°C and a 1 min extension at 72°C for 10 cycles followed by 30 s at 95°C, 30 s at 50°C and a 1 min extension at 72°C for 25 cycles. The MCT chimaeras were subsequently ligated into the pGHJ oocyte expression vector. For the MCT1/4 and MCT4/1 C-terminal chimaeras, the C-terminal regions were brought into the correct reading frame by a single base deletion and addition respectively using site-directed mutagenesis with the QuikChange[®] kit (Stratagene) as described previously [36]. Confirmation that chimaera constructs had been correctly engineered was provided by sequencing (The Sequencing Service, University of Dundee, Dundee, U.K.).

Measurement of MCT1 activity in rat erythrocytes

L-Lactate transport into rat erythrocytes was measured by monitoring the change in extracellular pH with a pH-sensitive electrode as described previously [37,38]. The cells were used at 3.5% or 7% haematocrit in lightly buffered saline medium supplemented with 5 μ M DIDS and 100 μ M acetazolamide to prevent bicarbonate/CO₂-mediated proton movements [37,38]. The erythrocytes were pre-incubated for 1 h at room temperature (22–25°C) with or without AR-C155858 at the required concentration prior to assaying lactate transport. This was performed at 6°C with substrate uptake initiated by addition of 10 mM L-lactate. Initial rates of transport were calculated by first-order regression analysis of the time course of pH change and converted into nmol of H⁺ per min by determining the pH change induced by small additions of standardized NaOH.

Measurement of MCT transport activity in *Xenopus* oocytes

cRNA was prepared by *in vitro* transcription from the appropriate linearized pGHJ plasmid (mMessage mMachine, Ambion) and injected into *X. laevis* oocytes as described previously [33]. For most assays 20 ng of cRNA was injected, but for [14 C] kinetic assays, injection quantity was adjusted to ensure

that uptake was linear with time. Further details can be found in Supplementary Table S2 (at <http://www.BiochemJ.org/bj/425/bj4250523add.htm>). Controls received the equivalent volume (9.2 nl) of water. Oocytes were then cultured in OR3 medium for 72 h with fresh medium each day. Rates of L-lactate transport by wild-type or chimaeric MCTs were determined as described previously, either by following the change in intracellular pH using the ratiometric pH-sensitive fluorescent dye BCECF [2'-7'-bis(carboxyethyl)-5(6)-carboxyfluorescein] [6,38] or by measuring uptake of [14 C] substrate (L-lactate or pyruvate) [33]. For measurement of AR-C155858 sensitivity, ten oocytes were placed in a six-well plate containing 5 ml of uptake buffer [75 mM NaCl, 2 mM KCl, 0.82 mM MgCl₂, 1 mM CaCl₂ and 20 mM Mes (pH 6.0)] and allowed to pre-incubate for the required time (usually 45 min) with or without AR-C155858 as required. Five oocytes were removed and placed into 50 μ l of uptake buffer containing L-[14 C]lactate (0.5 mM, 7.4 MBq/ml) with or without AR-C155858 at the required concentration. Incubation at room temperature was continued for the period over which uptake was linear with time; this varied with the construct employed, as detailed in Supplementary Table S2. The oocytes were then rapidly washed five times with ice-cold uptake buffer and, after the final wash, each egg was transferred into a scintillation vial and homogenized in 100 μ l of 2% (w/v) SDS by vigorous vortex-mixing. Scintillation fluid (10 ml of Emulsifier-Safe, PerkinElmer) was then added and [14 C] assayed by scintillation counting.

For the determination of K_m values for pyruvate and L-lactate, oocytes were equilibrated in incubation buffer [75 mM NaCl, 2 mM KCl, 0.82 mM MgCl₂, 1 mM CaCl₂ and 20 mM Tris/Hepes (pH 7.4)] for 5 min and then four oocytes incubated with 40 μ l of uptake buffer containing [14 C]-labelled L-lactate or pyruvate (7.4 MBq/ml) at a final concentration of 0.2, 0.5, 1, 2, 5, 20, 50 and 75 mM. Incubation was continued for the period over which uptake was linear with time (detailed in Supplementary Table S2), following which oocytes were washed and prepared for scintillation counting as above. Net MCT1-mediated uptake of L-lactate was determined by subtracting the uptake by water-injected oocytes determined at the same time.

MCT expression at the plasma membrane was confirmed by immunofluorescence microscopy of oocytes sectioned by embedding in chicken liver as described previously [33,39].

RESULTS

Determining the K_i of AR-C155858 for MCT1 in rat erythrocytes

Rat erythrocytes support very rapid lactate transport that is mediated by three mechanisms. The majority is via MCT1, but a small proportion may occur via the anion exchanger AE1 and by free diffusion of the undissociated lactic acid [26,40]. Transport mediated by AE1 can be blocked by 5 μ M DIDS, a concentration that has a minimal effect on MCT1 [37,38]. Using a pH electrode to determine the extracellular increase in pH that accompanies the proton-linked transport of 10 mM L-lactate into erythrocytes at 6°C we have investigated the inhibition of MCT1 by AR-C155858. It was first established that inhibition by low (nanomolar) concentrations of AR-C155858 reached equilibrium within 30–45 min incubation at room temperature (results not shown). Thus for detailed inhibitor titrations with increasing concentrations of AR-C155858 we used 60 min incubation of erythrocytes at both 3.5 and 7% haematocrit. After incubation with inhibitor at room temperature, cell suspensions were cooled to 6°C before measurement of L-lactate transport and determination of initial rates. In Figure 1 we show that the

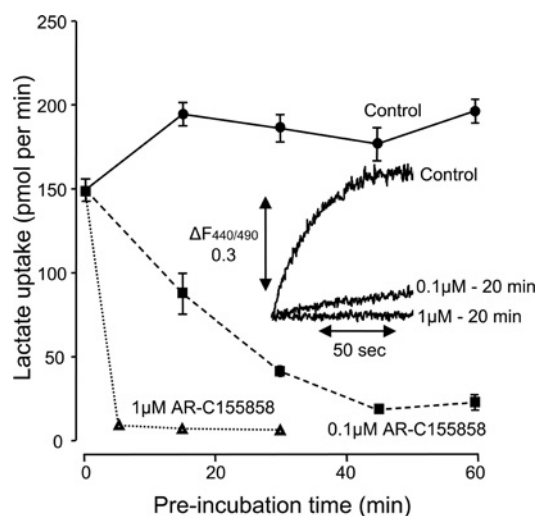


Figure 2 MCT1 expressed in *Xenopus* oocytes is inhibited by AR-C155858 in a time- and concentration-dependent manner

Xenopus oocytes were injected with the appropriate cRNA and after 72 h expression were pre-incubated in pH 6 oocyte transport buffer in the presence or absence of 0.1 μ M or 1 μ M AR-C155858 for the times shown. The uptake of 0.5 mM L-[14 C]lactate uptake was then determined after 2.5 min over which period it was found to be linear with time. Data are shown as means \pm S.E.M. of ten separate oocytes. The inset shows the uptake of 20 mM L-lactate measured at pH 6.0 using the pH-sensitive dye BCECF. Data are presented for the same oocyte in the absence of inhibitor and then after 20 min superfusion with 0.1 μ M and 1 μ M AR-C155858.

concentration-dependence of inhibition is almost linear up to 80% inhibition, as predicted for a very tight-binding inhibitor whose concentration is less than the concentration of the target protein (MCT1). By performing parallel experiments at two cell densities (3.5% and 7% haematocrit) the data can be fitted by non-linear regression analysis to the equation for a tight-binding non-competitive inhibitor using the total inhibitor concentration and the haematocrit as the two x -variables [41,42]. This allowed us to determine values (\pm S.E. for the fit shown) for the K_i (2.3 ± 1.4 nM), the number of binding sites (E_t) for AR-C155858 inhibition (1.29 ± 0.09 nmol per ml of packed cells) and the turnover number (k_{cat}) of MCT1 in rat erythrocytes (12.2 ± 1.1 s⁻¹).

Time- and concentration-dependence of MCT inhibition by AR-C155858 in *Xenopus* oocytes

In order to perform accurate comparisons of the affinity of the different MCT isoforms towards AR-C155858 we expressed MCT1, MCT2 and MCT4 in *X. laevis* oocytes. It was first necessary to ensure that the time of incubation of oocytes with inhibitor was sufficient to allow compound binding to the MCT to reach equilibrium. In Figure 2 the rate of [14 C]lactate uptake into MCT1-expressing oocytes was determined after incubation with 0.1 μ M AR-C155858 for 15, 30, 45 and 60 min. For each time point, mean data (\pm S.E.M) for ten separate oocytes are presented. The data show that, as with the erythrocytes, 45 min incubation with inhibitor was sufficient to give maximal inhibition. As might be predicted, with 1 μ M AR-C155858 inhibition occurred much more quickly and was almost maximal at 5 min. This was confirmed by BCECF assay of transport as shown in the inset to Figure 2. From these data we chose to use a 45 min incubation time for comparing the relative potency of AR-C155858 as an inhibitor of MCT1, MCT2 and MCT4. In Figure 3 we show that the concentration-dependence of MCT1 follows a linear trend up to 30 nM (70% inhibition) and then curves off towards 100%

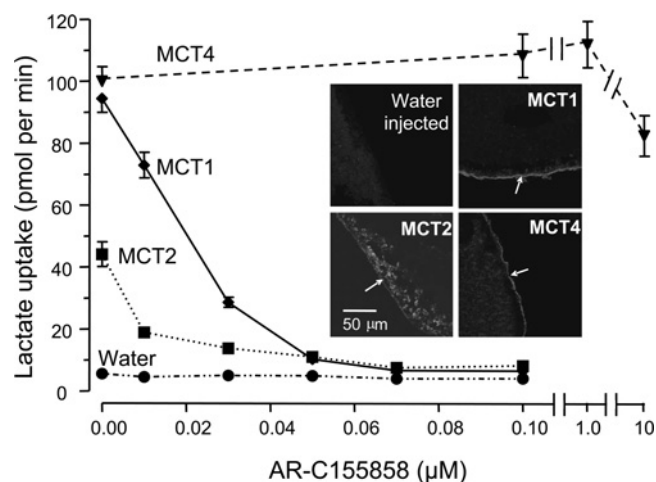


Figure 3 When expressed in *Xenopus* oocytes, MCT1 and MCT2, but not MCT4, are sensitive to inhibition by AR-C155858

Xenopus oocytes were injected with appropriate cRNA or water and after 72 h expression they were incubated with the concentration of AR-C155858 shown for 45 min prior to measurement of L-[¹⁴C]lactate uptake over 2.5 min. Data are shown as the means \pm S.E.M. of 15–40 separate oocytes for each inhibitor concentration. The inset images show the expression of the relevant MCT in oocyte sections revealed using immunofluorescence microscopy with C-terminal antibodies against the relevant MCT. Arrows indicate the location of the plasma membrane. Note that for MCT2 a significant proportion of the MCT remains in an intracellular compartment.

inhibition at 100 nM. Again, this behaviour is that predicted for a very high-affinity inhibitor and thus consistent with the K_i for AR-C155858 of 2.3 nM determined using rat erythrocytes. By contrast, oocytes expressing MCT4 at levels supporting similar rates of lactate transport revealed no significant inhibition by 1 μ M AR-C155858, and even at 10 μ M AR-C155858 inhibition was only approx. 20%. In oocytes expressing MCT2 the initial rate of transport was less than for MCT1 and MCT4, consistent with the poorer expression of MCT2 at the plasma membrane as reported previously [38]. This is a consequence of MCT2 binding less well to the endogenous basigin expressed by *Xenopus* oocytes than does MCT1 and MCT4 [38,43]. Nevertheless, it is clear that MCT2 is potently inhibited by AR-C155858, and the 70% inhibition seen at 10 nM is followed by a gradually increasing inhibition which can only be explained by a K_i value of significantly less than 10 nM.

Extrapolation of the linear portion of the plot shown for MCT1 inhibition to zero carrier-mediated rate (i.e. water-injected rate) provided an estimated concentration of MCT1 in the incubation of 40 nM. Each egg was incubated in 10 μ l so this represents 0.4 pmol of MCT1 per egg. The rate of L-lactate uptake was approx. 95 pmol/egg per min which gives a turnover number of 4 s⁻¹ for MCT1 in oocytes at 22°C with 0.5 mM L-lactate. Since the initial slope of the inhibitor plot for MCT2 cannot be accurately determined, it is not possible to determine an accurate turnover number for this isoform. Nevertheless, linear extrapolation of the plot would give a maximal value for the concentration of MCT2 to be approx. 15 nM, corresponding to a maximal expression of MCT2 of 0.15 pmol per egg. This would yield a minimum estimate of the turnover number for MCT2 in oocytes at 22°C with 0.5 mM L-lactate of 5 s⁻¹, which is similar to MCT1.

AR-C155858 probably binds to MCT1 from the cytosolic side

The slow time-dependence of inhibition by AR-C155858 could reflect slow binding to a site on the external surface or perhaps,

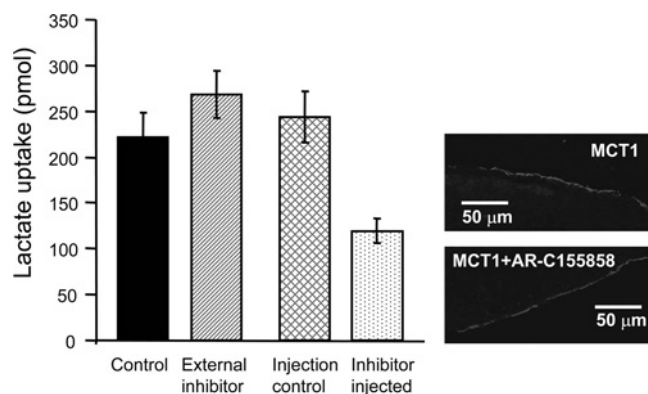


Figure 4 Microinjection of AR-C155858 inhibits MCT1 expressed in *Xenopus* oocytes

MCT1 was expressed in *Xenopus* oocytes for 72 h prior to inhibitor treatment and assay of L-[¹⁴C]lactate uptake over 2.5 min. For addition of AR-C155858 internally, 20 oocytes were individually injected with 9.2 nl of 1 mM AR-C155858 or DMSO as a control, incubated for 5 min in 5 ml of pH 6 transport buffer and washed once prior to transport assay. For incubation with the equivalent amount of AR-C155858 added externally, 20 aliquots (9.2 nl) of 1 mM AR-C155858 were added to 5 ml of pH 6 transport buffer (final concentration of 35 nM) and incubated with the oocytes for 5 min prior to a single wash and transport assay as above. Uptake was corrected for the uptake by water-injected eggs under the same conditions and are presented as means \pm S.E.M. of 18–20 separate oocytes. The two images on the right-hand side show the plasma membrane expression of MCT1 in control oocytes and those incubated for 1 h with 1 μ M AR-C155858 revealed by immunofluorescence microscopy.

more likely, a slow permeation of the inhibitor into the cell where it binds to an internal site on MCT1. In order to discriminate between the two possibilities we microinjected 9.2 nl of 1 mM AR-C155858 into oocytes, corresponding to a total internal concentration of approx. 23 μ M (assuming an internal volume of 0.4 μ l per egg [44] and ignoring binding to intracellular components). Each oocyte (20 in total) was immediately transferred into 5 ml of pH 6 transport buffer and then left for 5 min prior to washing once and determining the rate of L-[¹⁴C]lactate uptake. As a control, the same quantity of inhibitor (184 nl corresponding to 20 oocytes worth of inhibitor) was added to 5 ml of buffer (36.8 nM final) prior to addition of 20 oocytes and 5 min incubation. These oocytes were subsequently washed and transport determined as for AR-C155858-injected oocytes. As an additional control, some oocytes were injected with 9.2 nl of DMSO. The results in Figure 4 show that the rate of L-lactate uptake was approx. 50% inhibited in the AR-C155858-injected oocytes, whereas the same quantity of inhibitor added outside was without effect. It might also be argued that the slow time course of inhibition could reflect internalization of MCT1. However, the immunofluorescence results in Figure 4 confirm that the expression of MCT1 at the plasma membrane was unchanged in oocytes incubated with 1 μ M AR-C155858 for 1 h to give full inhibition of transport.

AR-C155858 inhibition involves TM helices 7–10 in the C-terminal half of MCT1

Since MCT1 is inhibited by AR-C155858, whereas MCT4 is not, we made MCT1/4 chimaeras to establish the region on MCT1 to which the inhibitor binds. The structures of these MCT1/4 chimaeras are shown schematically in (A) of each relevant Figure. We first created chimaeras in which the N-terminal half and large intracellular loop were of MCT1 and the C-terminal half was from MCT4. This chimaera (MCT1/4) was expressed at the plasma membrane of oocytes and transported L-lactate, albeit at a greatly reduced rate (Figure 5B). However, like MCT4, it was insensitive

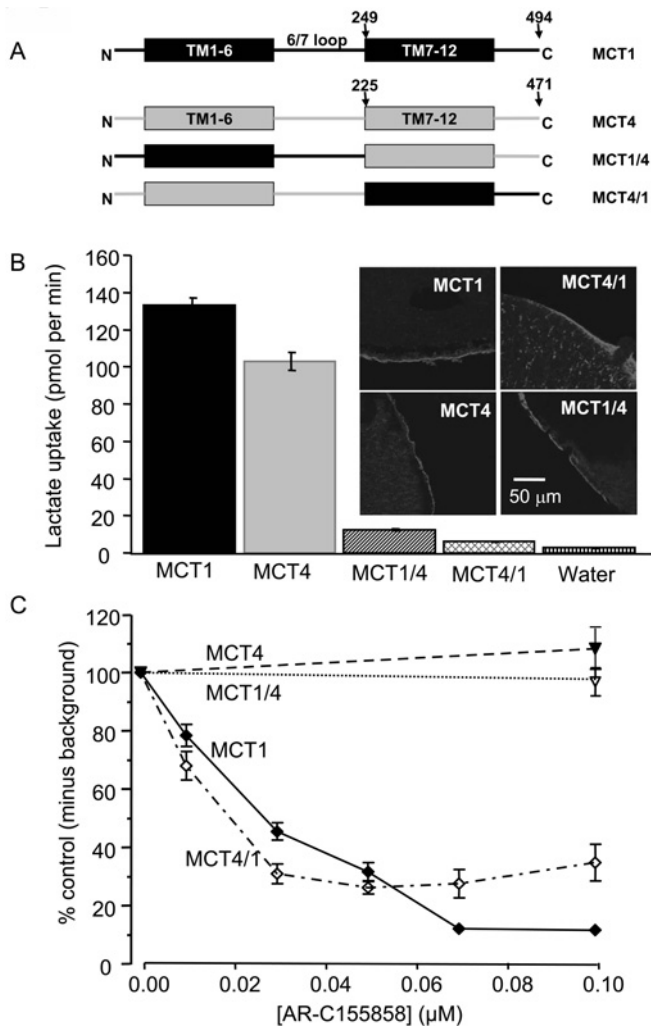


Figure 5 The binding site of MCT1 for AR-C155858 resides within the C-terminal half of the transporter

(A) Shows a schematic of the MCT1/4 and MCT4/1 chimaeras used, with MCT1 sequence being shown in black and MCT4 sequence in grey. The numbered arrows indicate the position that the switch was made between MCT1 and MCT4. Native and chimaeric MCTs were expressed in oocytes for 72 h prior to incubation with AR-C155858 after which assay of L-[¹⁴C]lactate uptake was determined as described in Figures 2 and 3. Note that different times of uptake were employed depending on the activity of the chimaera as detailed in Supplementary Table S2 (at <http://www.BiochemJ.org/bj/425/bj4250523add.htm>). (B) Data on the absolute rate of transport of each chimaera in the absence of inhibitor. (C) The activity at each inhibitor concentration expressed as a percentage of the uninhibited rate, after the background uptake rate of water-injected oocytes was subtracted. Data are shown as the means \pm S.E.M. of 20–50 separate oocytes for each condition. The inset images of (B) show the plasma membrane expression of each native and chimaeric MCT revealed by immunofluorescence microscopy.

to inhibition by AR-C155858 (Figure 5C). We also made the reverse chimaera MCT4/1. It too was expressed at the plasma membrane, although there appeared to be a significant amount of the chimaera that was in a vesicular compartment and not at the plasma membrane (Figure 5B). Nevertheless, this MCT4/1 chimaera showed a sensitivity to AR-C155858 similar to MCT1 (Figure 5C). Thus our results imply that the binding site of MCT1 for AR-C155858 is contained within the C-terminal half of the molecule, beyond the intracellular loop between TMs 6 and 7.

In order to define the binding site of the inhibitor more precisely we created additional chimaeras. We first made chimaeras in which either the C-terminal tail of MCT1 was removed or swapped

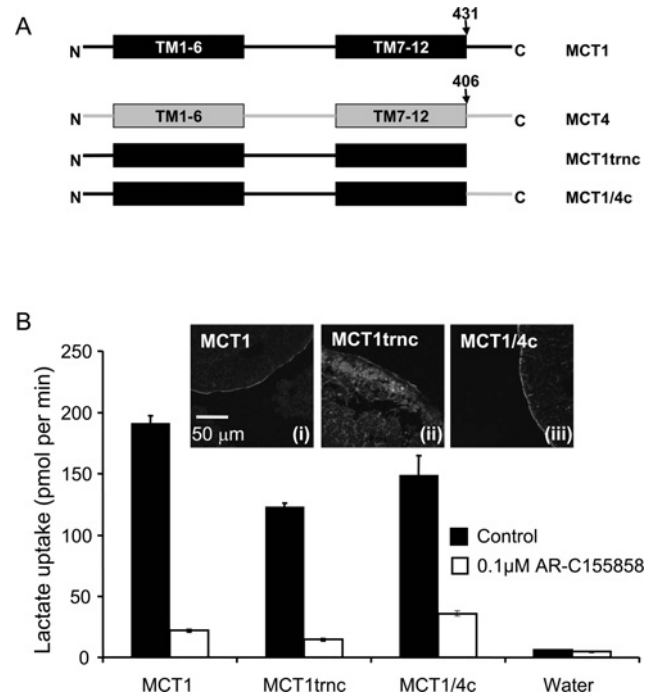


Figure 6 The C-terminus of MCT1 is not involved in AR-C155858 sensitivity

(A) Shows a schematic of the MCT1/4 and MCT4/1 chimaeras used, with MCT1 sequence being shown in black and MCT4 sequence in grey. The numbered arrows indicate the position that the switch was made between MCT1 and MCT4. Native and chimaeric MCTs were expressed in oocytes for 72 h prior to incubation with or without 0.1 μM AR-C155858 for 45 min, after which assay of L-[¹⁴C]lactate uptake was determined over 2.5 min as described in Figures 2 and 3. (B) Provides mean data (\pm S.E.M. for ten oocytes) on the absolute rate of transport of each chimaera in the absence and presence of inhibitor. The inset images show the plasma membrane expression of each native and chimaeric MCT revealed by immunofluorescence microscopy.

for that of MCT4 as shown schematically in Figure 6(A). Both the MCT1trnc and MCT1/4c were expressed at the plasma membrane of oocytes, although a significant amount of MCT1trnc remained intracellular. Nevertheless, this chimaera still transported lactate with rates similar to that seen with normal MCT1 and MCT4. Although we did not perform detailed inhibitor titrations we showed that both the MCT1/4c chimaera and MCT1trnc were strongly inhibited by 0.1 μM AR-C155858, like MCT1 itself. These results imply that the binding site for AR-C155858 does not require the C-terminal tail of MCT1. In order to establish which of the C-terminal TM helices might be important for inhibitor binding we compared the C-terminal TM sequences of MCT1, MCT2 and MCT4 and found that it was within TM11 that MCT4 (inhibitor-insensitive) exhibited the greatest difference to MCT1 and MCT2 (inhibitor-sensitive). Thus we made chimaeras in which the switch between MCT1 and MCT4 was performed at the start of TM11. Unfortunately, as shown in the inset to Figure 7(B), the MCT1/4TM11 chimaera was not expressed properly at the plasma membrane and no enhancement of L-lactate transport over water-injected eggs was detected. However, the MCT4/1TM11 chimaera was expressed at the plasma membrane and did transport L-lactate, albeit very slowly (Figure 7B). Subtraction of the very low background rate of lactate transport by uninjected oocytes, which was inhibited by AR-C155858, revealed that the residual lactate transport activity mediated by MCT4/1TM11 was insensitive to inhibition by AR-C155858. This suggests that the binding site for AR-C155858 does not involve TMs 11 and 12 as we had initially reasoned and must therefore involve TMs 7–10.

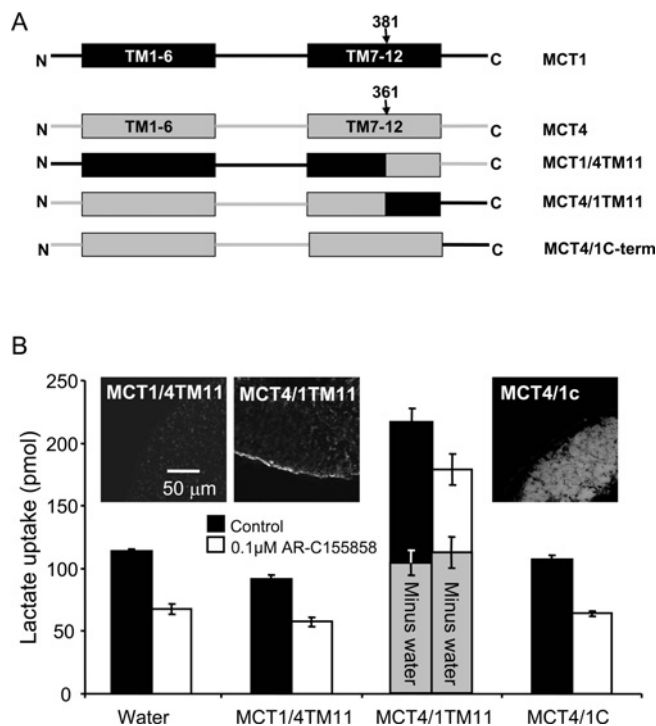


Figure 7 A region within TMs 7–10 of MCT1 is required for sensitivity to AR-C155858

(A) Shows a schematic of the MCT1/4 and MCT4/1 chimaeras used, with MCT1 sequence being shown in black and MCT4 sequence in grey. The numbered arrows indicate the position that the switch was made between MCT1 and MCT4. Native and chimaeric MCTs were expressed in oocytes for 72 h prior to incubation with or without 0.1 μ M AR-C155858 for 45 min, after which assay of L-[14 C]lactate uptake was determined over 1 h. This prolonged uptake period was required because of the low rates of transport being measured. (B) Provides mean data (\pm S.E.M. for ten oocytes) on the absolute rate of transport of each chimaera in the absence and presence of inhibitor. The inset images show the plasma membrane expression of each native and chimaeric MCT revealed by immunofluorescence microscopy.

Kinetic properties of the MCT1/4 and MCT4/1 chimaeras

The relatively low rates of transport seen with the MCT4/1 and MCT1/4 chimaeras may reflect a high K_m for L-lactate and thus low rates of transport when measured at 0.5 mM L-lactate. In order to investigate this possibility, and to provide some clues as to how the two halves of the MCT might be involved in substrate binding, the K_m values of the chimaeras for L-lactate and pyruvate were determined (Table 1). The MCT4/1 chimaera exhibited a K_m value for L-lactate of 15–25 mM, depending on whether the BCECF or

Table 1 K_m values of MCT chimaeras for L-lactate and pyruvate

The K_m values reported were derived using either L-[14 C]lactate uptake or by monitoring changes in intracellular pH with BCECF as described in the Experimental section. Data are given \pm S.E.M. derived from the fit of the mean data to the Michaelis–Menten equation by non-linear least squares analysis. The n values given represent the number of separate eggs used for each substrate concentration. No L-[14 C]lactate uptake data are provided for the MCT4/1 chimaera because the very high K_m values required the use of high substrate concentrations for which the specific activity became too low to measure uptake of L-[14 C]lactate accurately.

MCT form	K_m value (mM) using [14 C] substrate		K_m value (mM) using BCECF	
	Lactate	Pyruvate	Lactate	Pyruvate
MCT1	5.7 \pm 1.2 (n = 16)	1.2 \pm 0.2 (n = 16)	3.5*	1*
MCT4	12.9 \pm 2 (n = 16)	103 \pm 28 (n = 24)	28*	150*
MCT1/4	26.5 \pm 5.7 (n = 16)	8.9 \pm 2 (n = 16)	15.8 \pm 2.6 (n = 7)	8.5 \pm 1.9 (n = 9)
MCT4/1	–	–	209.2 \pm 71.9 (n = 7)	27.3 \pm 5.2 (n = 8)

*BCECF data for MCT1 and MCT4 are taken from [6].

radioactive assay was used, whereas both techniques gave a K_m value for pyruvate of 8–9 mM. These K_m values are similar to that of MCT4 in the case of L-lactate, but intermediate between MCT1 and MCT4 for pyruvate. In the case of the MCT4/1 chimaera, K_m values were too high to be determined radioactively, but using BCECF they were found to be 209 \pm 72 mM for L-lactate and 27 \pm 5 mM for pyruvate. Thus with this chimaera also, the K_m for pyruvate was intermediate between MCT1 and MCT4, whereas the K_m for L-lactate was much higher than that for either isoform.

DISCUSSION

Previously, a new class of specific and extremely potent inhibitors of MCT1 have been discovered by AstraZeneca that were reported to show no binding to MCT4 and exhibit lower-affinity binding to MCT2 [30–32]. The K_d values for these inhibitors binding to endogenous MCT1 in rat and human cells was found to be in the low nanomolar region or less, as was also found for MCT1 expressed in Ins-1 cells that contain little or no endogenous MCT1 [30,31]. Similar K_d values were determined for MCT1 expressed in yeast [30], and the K_i value of AR-C155858 for MCT1 we have determined in rat erythrocytes of 2.3 \pm 1.4 nM is entirely consistent with the K_i of 1.2 nM for binding of AR-C155858 to human erythrocyte MCT1 derived from radioligand-binding experiments [45].

The turnover number for MCT1 can be calculated using AR-C155858

The inhibitor titration in rat erythrocytes has allowed us to determine the concentration of MCT1 in these cells to be 1.29 \pm 0.09 nmol per ml of packed cells. Since the number of erythrocytes in 1 ml of packed blood is known to be approx. 10^{10} [26] it is possible to calculate that there are approx. 80 000 molecules of MCT1 per rat erythrocyte. This value is quite similar to the value of 46 000 \pm 11 000 determined previously by [3 H] inhibitor binding [30] and represents approx. 8% of the value for the anion exchanger AE1 [26]. Using the rate of L-lactate transport and the concentration of MCT1 we calculated the turnover number (k_{cat}) to be 12.2 \pm 1.1 s $^{-1}$ at 6°C. Since we have previously determined the temperature-dependence of MCT1 [29], we are able to calculate that the rate of L-lactate transport by rat erythrocytes at room temperature will be approx. 7-fold higher than at 6°C. This would bring the predicted turnover number for MCT1 in rat erythrocytes to approx. 85 s $^{-1}$ which is similar to the value of 35 s $^{-1}$ determined for the glucose transporter GLUT1 in rat erythrocytes at 20°C [46,47], but approx. 5-fold less than the k_{cat} determined for endogenous

human GLUT1 in erythrocytes or when overexpressed in *Xenopus* oocytes [48].

When expressed in *Xenopus* oocytes, MCT1 also showed time-dependent inhibition by AR-C155858 (Figure 2) with the extent of inhibition being linear with respect to AR-C155858 concentrations up to approx. 70% inhibition (Figure 3). This is consistent with a very low (nanomolar) K_i value determined in erythrocytes. By extrapolation of the linear portion of the inhibitor titration we were able to estimate that the amount of MCT1 expressed at the plasma membrane was approx. 0.4 pmol per oocyte. From this value and the rate of lactate transport, the turnover number of MCT1 in oocytes at 22°C was calculated to be 4 s⁻¹. However, this value was determined at 0.5 mM L-lactate and thus cannot be compared directly with the value of 85 s⁻¹ calculated for rat erythrocytes at 22°C with 10 mM L-lactate. The K_m for MCT1 in erythrocytes and oocytes is approx. 3.5 mM [6,29], and thus from Michaelis–Menten kinetics the rate of transport at 10 mM L-lactate would be predicted to be 6-fold higher than at 0.5 mM. This would increase the turnover number of MCT1 in oocytes to 24 s⁻¹, which is approx. 30% of the value determined for MCT1 in erythrocytes. However, we have shown previously that the rate of L-lactate uptake by oocytes determined radioactively underestimates the true transport rate determined with BCECF [6]. This is because of an unstirred layer effect that slows diffusion of L-[¹⁴C]lactate taken up into the body of the oocyte. Thus overall there is reasonable agreement between the values measured in erythrocytes and oocytes.

AR-C155858 is a potent inhibitor of MCT1 and MCT2, but not MCT4

In agreement with competition-binding studies of MCTs expressed in yeast for related compounds [30], we have shown that AR-C155858 inhibits both MCT1 and MCT2, but not MCT4 when expressed in oocytes (Figure 3). Although we were unable to determine an accurate K_i value for inhibition of MCT2 by AR-C155858, we can conclude from the shape of the inhibitor titration that the value must be significantly less than 10 nM. In previous studies of inhibitor binding to MCT1 and MCT2 expressed in yeast, K_d values of 4.9 and 100 nM respectively were determined (P. A. Rugman, A. P. Jackson and C. M. Murray, unpublished work). For MCT1 this represents a reasonable agreement with the K_i values for endogenous MCT1 in rat and human cells derived in the present study and previously [44]. However, this is not the case for MCT2 where the yeast binding data suggest that the affinity of MCT2 for AR-C155858 is more than an order of magnitude less than for MCT1. One explanation for this difference may be the absence of either basigin or embigin when MCTs are expressed in yeast, and this might affect inhibitor binding. In this context it may be noted that inhibition of MCT1 and MCT2 by the organomercurial reagent p-chloromercuribenzenesulfonate also depends on the associated ancillary protein [38]. Our results would also imply that interpretation of metabolic studies in which AR-C122982 has been used to discriminate between MCT1- and MCT2-mediated lactate transport [49] may not be straightforward.

The binding site for AR-C155858 involves TMs 7–10 of MCT1, and probably faces the cytosol

The use of MCT1/MCT4 chimaeric transporters reveals that the binding site for AR-C155858 is contained within the C-terminal half of the transporter. Thus MCT1/4, like MCT4, was insensitive to inhibition by AR-C155858, whereas MCT4/1 was inhibitor-sensitive, like MCT1 (Figure 5). The C-terminal tail of MCT1 appears to have no major effect on the sensitivity to inhibition

by AR-C155858 since potent inhibition by AR-C155858 was still observed when it was either removed or replaced with the tail of MCT4 (Figure 6). However, the chimaera containing TMs 1–10 of MCT4 and TMs 11 and 12 plus the C-terminal tail of MCT1 was insensitive to AR-C155858 (Figure 7). These results demonstrate that the binding site for AR-C155858 is contained, at least in part, within TMs 7–10 of MCT1. The slow time-dependence of inhibition by AR-C155858 (Figure 2) could be explained either by the inhibitor having to enter the cell before binding to an intracellular site on MCT1 or by internalization of MCT1 upon inhibitor binding. However, we showed that no MCT1 internalization occurred, even at full inhibition, and that the inhibitor worked well if microinjected into oocytes (Figure 4). These results imply that the binding site for AR-C155858 probably faces the cytosol, where our molecular model of MCT1 predicts TMs 7 and 10 to form part of the inward facing substrate-binding pocket [33,36]. This is also consistent with earlier observations that Phe³⁶⁰ in TM10 is involved in substrate binding since its mutation to cysteine allows MCT1 to accommodate the larger monocarboxylate mevalonate [7,50]. Furthermore, we have previously shown that Asp³⁰² and Arg³⁰⁶ in TM8 are critical residues in the translocation cycle. However, analysis of the kinetics of MCT1/4 and MCT4/1 chimaeras suggest that substrate binding may not be exclusively located within the C-terminal half of MCT1. Thus both the C- and N-terminal halves of the MCT influence the kinetics of transport (Table 1). This is entirely consistent with our recent molecular model of MCT1 which predicts that the substrate-binding pocket and translocation channel involve helices from both the C- and N-terminal domains with critical roles for Lys³⁸ in TM1, and Asp³⁰² plus Arg³⁰⁶ in TM8 [33,36].

AUTHOR CONTRIBUTION

Matthew Ovens performed the oocyte studies, Andrew Davies the erythrocyte work and Marieangela Wilson provided molecular biological expertise especially for the creation of chimaeric transporters. Clare Murray advised on the use of AR-C155858 whereas Andrew Halestrap directed the research and wrote the manuscript with assistance from Matthew Ovens and Clare Murray.

ACKNOWLEDGEMENTS

We thank Agnieszka Bierzynska for skilled technical support.

FUNDING

This work was supported by The Wellcome Trust [Project Grant number 079792/z/06/]; and the Medical Research Council (Ph.D. studentship to M.J.O.).

REFERENCES

- Halestrap, A. P. and Meredith, D. (2004) The SLC16 gene family: from monocarboxylate transporters (MCTs) to aromatic amino acid transporters and beyond. *Pflügers Arch.* **447**, 619–628
- Bröer, S., Schneider, H. P., Bröer, A., Rahman, B., Hamprecht, B. and Deitmer, J. W. (1998) Characterization of the monocarboxylate transporter 1 expressed in *Xenopus laevis* oocytes by changes in cytosolic pH. *Biochem. J.* **333**, 167–174
- Bröer, S., Bröer, A., Schneider, H. P., Stegen, C., Halestrap, A. P. and Deitmer, J. W. (1999) Characterization of the high-affinity monocarboxylate transporter MCT2 in *Xenopus laevis* oocytes. *Biochem. J.* **341**, 529–535
- Grollman, E. F., Philp, N. J., McPhie, P., Ward, R. D. and Sauer, B. (2000) Determination of transport kinetics of chick MCT3 monocarboxylate transporter from retinal pigment epithelium by expression in genetically modified yeast. *Biochemistry* **39**, 9351–9357
- Dimmer, K. S., Friedrich, B., Lang, F., Deitmer, J. W. and Bröer, S. (2000) The low-affinity monocarboxylate transporter MCT4 is adapted to the export of lactate in highly glycolytic cells. *Biochem. J.* **350**, 219–227

- 6 Manning Fox, J. E., Meredith, D. and Halestrap, A. P. (2000) Characterisation of human monocarboxylate transporter 4 substantiates its role in lactic acid efflux from skeletal muscle. *J. Physiol.* **529**, 285–293
- 7 Kim-Garcia, C., Goldstein, J. L., Pathak, R. K., Anderson, R. G. W. and Brown, M. S. (1994) Molecular characterization of a membrane transporter for lactate, pyruvate, and other monocarboxylates: implications for the Cori cycle. *Cell* **76**, 865–873
- 8 McCullagh, K. J. A., Poole, R. C., Halestrap, A. P., O'Brien, M. and Bonen, A. (1996) Role of the lactate transporter (MCT1) in skeletal muscles. *Am. J. Physiol.* **271**, E143–E150
- 9 Jackson, V. N., Price, N. T., Carpenter, L. and Halestrap, A. P. (1997) Cloning of the monocarboxylate transporter isoform MCT2 from rat testis provides evidence that expression in tissues is species-specific and may involve post-transcriptional regulation. *Biochem. J.* **324**, 447–453
- 10 Halestrap, A. P., Wang, X. M., Poole, R. C., Jackson, V. N. and Price, N. T. (1997) Lactate transport in heart in relation to myocardial ischemia. *Am. J. Cardiol.* **80**, A17–A25
- 11 Halestrap, A. P. and Price, N. T. (1999) The proton-linked monocarboxylate transporter (MCT) family: structure, function and regulation. *Biochem. J.* **343**, 281–299
- 12 Poole, R. C. and Halestrap, A. P. (1994) N-Terminal protein sequence analysis of the rabbit erythrocyte lactate transporter suggests identity with the cloned monocarboxylate transport protein MCT1. *Biochem. J.* **303**, 755–759
- 13 Garcia, C. K., Brown, M. S., Pathak, R. K. and Goldstein, J. L. (1995) cDNA cloning of MCT2, a second monocarboxylate transporter expressed in different cells than MCT1. *J. Biol. Chem.* **270**, 1843–1849
- 14 Pierre, K. and Pellerin, L. (2005) Monocarboxylate transporters in the central nervous system: distribution, regulation and function. *J. Neurochem.* **94**, 1–14
- 15 Bergersen, L. H. (2007) Is lactate food for neurons? Comparison of monocarboxylate transporter subtypes in brain and muscle. *Neuroscience* **145**, 11–19
- 16 Yoon, H. Y., Fanelli, A., Grollman, E. F. and Philp, N. J. (1997) Identification of a unique monocarboxylate transporter (MCT3) in retinal pigment epithelium. *Biochem. Biophys. Res. Commun.* **234**, 90–94
- 17 Philp, N. J., Yoon, H. Y. and Lombardi, L. (2001) Mouse MCT3 gene is expressed preferentially in retinal pigment and choroid plexus epithelia. *Am. J. Physiol. Cell Physiol.* **280**, C1319–C1326
- 18 Wilson, M. C., Jackson, V. N., Heddle, C., Price, N. T., Pilegaard, H., Juel, C., Bonen, A., Montgomery, I., Hutter, O. F. and Halestrap, A. P. (1998) Lactic acid efflux from white skeletal muscle is catalyzed by the monocarboxylate transporter isoform MCT3. *J. Biol. Chem.* **273**, 15920–15926
- 19 Juel, C. and Halestrap, A. P. (1999) Lactate transport in skeletal muscle: role and regulation of the monocarboxylate transporter. *J. Physiol.* **517**, 633–642
- 20 Ullah, M. S., Davies, A. J. and Halestrap, A. P. (2006) The plasma membrane lactate transporter MCT4, but not MCT1, is up-regulated by hypoxia through a HIF-1 α -dependent mechanism. *J. Biol. Chem.* **281**, 9030–9037
- 21 Poole, R. C. and Halestrap, A. P. (1993) Transport of lactate and other monocarboxylates across mammalian plasma membranes. *Am. J. Physiol.* **264**, C761–C782
- 22 Meredith, D. and Christian, H. C. (2008) The SLC16 monocarboxylate transporter family. *Xenobiotica* **38**, 1072–1106
- 23 Sonveaux, P., Vegran, F., Schroeder, T., Wergin, M. C., Verrax, J., Rabbani, Z. N., De Saedeleer, C. J., Kennedy, K. M., Diepart, C., Jordan, B. F. et al. (2008) Targeting lactate-fueled respiration selectively kills hypoxic tumor cells in mice. *J. Clin. Invest.* **118**, 3930–3942
- 24 Fang, J., Quinones, Q. J., Holman, T. L., Morowitz, M. J., Wang, Q., Zhao, H., Sivo, F., Maris, J. M. and Wahl, M. L. (2006) The H⁺-linked monocarboxylate transporter (MCT1/SLC16A1): a potential therapeutic target for high-risk neuroblastoma. *Mol. Pharmacol.* **70**, 2108–2115
- 25 Erlichman, J. S., Hewitt, A., Damon, T. L., Hart, M., Kurascz, J., Li, A. and Leiter, J. C. (2008) Inhibition of monocarboxylate transporter 2 in the retrotrapezoid nucleus in rats: a test of the astrocyte-neuron lactate-shuttle hypothesis. *J. Neurosci.* **28**, 4888–96
- 26 Halestrap, A. P. (1976) Pyruvate and lactate transport into human erythrocytes. Evidence for the involvement of the chloride carrier and a chloride independent carrier. *Biochem. J.* **156**, 193–207
- 27 Halestrap, A. P. and Denton, R. M. (1974) Specific inhibition of pyruvate transport in rat liver mitochondria and human erythrocytes by α -cyano-4-hydroxycinnamate. *Biochem. J.* **138**, 313–316
- 28 Halestrap, A. P. (1975) The mitochondrial pyruvate carrier: kinetics and specificity for substrates and inhibitors. *Biochem. J.* **148**, 85–96
- 29 Carpenter, L. and Halestrap, A. P. (1994) The kinetics, substrate and inhibitor specificity of the lactate transporter of Ehrlich-Lettre tumour cells studied with the intracellular pH indicator BCECF. *Biochem. J.* **304**, 751–760
- 30 Murray, C. M., Hutchinson, R., Bantick, J. R., Belfield, G. P., Benjamin, A. D., Brazma, D., Bundick, R. V., Cook, I. D., Craggs, R. I., Edwards, S. et al. (2005) Monocarboxylate transporter MCT1 is a target for immunosuppression. *Nat. Chem. Biol.* **1**, 371–376
- 31 Guile, S. D., Bantick, J. R., Cheshire, D. R., Cooper, M. E., Davis, A. M., Donald, D. K., Evans, R., Eyssade, C., Ferguson, D. D., Hill, S. et al. (2006) Potent blockers of the monocarboxylate transporter MCT1: novel immunomodulatory compounds. *Bioorg. Med. Chem. Lett.* **16**, 2260–2265
- 32 Ekberg, H., Qi, Z., Pahlman, C., Veress, B., Bundick, R. V., Craggs, R. I., Holness, E., Edwards, S., Murray, C. M., Ferguson, D. et al. (2007) The specific monocarboxylate transporter-1 (MCT-1) inhibitor, AR-C117977, induces donor-specific suppression, reducing acute and chronic allograft rejection in the rat. *Transplantation* **84**, 1191–1199
- 33 Manoharan, C., Wilson, M. C., Sessions, R. B. and Halestrap, A. P. (2006) The role of charged residues in the transmembrane helices of monocarboxylate transporter 1 and its ancillary protein basigin in determining plasma membrane expression and catalytic activity. *Mol. Membr. Biol.* **23**, 486–498
- 34 Poole, R. C., Sansom, C. E. and Halestrap, A. P. (1996) Studies of the membrane topology of the rat erythrocyte H⁺/lactate cotransporter (MCT1). *Biochem. J.* **320**, 817–824
- 35 Choi, M. Y., Fuerst, M. J., Rafaelli, A. and Jurenka, R. Role of extracellular domains in PBAN/pyrokinin GPCRs from insects using chimera receptors. *Insect Biochem. Mol. Biol.* **37**, 296–306
- 36 Wilson, M. C., Meredith, D., Bunnun, C., Sessions, R. B. and Halestrap, A. P. (2009) Studies on the DIDS binding site of monocarboxylate transporter 1 suggest a homology model of the open conformation and a plausible translocation cycle. *J. Biol. Chem.* **284**, 20011–20021
- 37 Poole, R. C. and Halestrap, A. P. (1991) Reversible and irreversible inhibition, by stilbenedisulphonates, of lactate transport into rat erythrocytes: identification of some new high-affinity inhibitors. *Biochem. J.* **275**, 307–312
- 38 Wilson, M. C., Meredith, D., Fox, J. E. M., Manoharan, C., Davies, A. J. and Halestrap, A. P. (2005) Basigin (CD147) is the target for organomercurial inhibition of monocarboxylate transporter isoforms 1 and 4: the ancillary protein for the insensitive MCT2 is embigin (Gp70). *J. Biol. Chem.* **280**, 27213–27221
- 39 Friesema, E. C. H., Ganguly, S., Abdalla, A., Fox, J. E. M., Halestrap, A. P. and Visser, T. J. (2003) Identification of monocarboxylate transporter 8 as a specific thyroid hormone transporter. *J. Biol. Chem.* **278**, 40128–40135
- 40 Deuticke, B., Beyer, E. and Forst, B. (1982) Discrimination of three parallel pathways of L-lactate transport in the human erythrocyte membrane by inhibitors and kinetic properties. *Biochim. Biophys. Acta* **684**, 96–110
- 41 Shearman, M. S. and Halestrap, A. P. (1984) The concentration of the mitochondrial pyruvate carrier in rat liver and heart mitochondria determined with α -cyano- β -(1-phenylindol-3-yl)acrylate. *Biochem. J.* **223**, 673–676
- 42 Davidson, A. M. and Halestrap, A. P. (1990) Partial inhibition by cyclosporin A of the swelling of liver mitochondria *in vivo* and *in vitro* induced by sub-micromolar [Ca²⁺] but not by butyrate: evidence for two distinct swelling mechanisms. *Biochem. J.* **268**, 147–152
- 43 Kirk, P., Wilson, M. C., Heddle, C., Brown, M. H., Barclay, A. N. and Halestrap, A. P. (2000) CD147 is tightly associated with lactate transporters MCT1 and MCT4 and facilitates their cell surface expression. *EMBO J.* **19**, 3896–3904
- 44 Stegen, C., Matskevich, I., Wagner, C. A., Paulmichl, M., Lang, F. and Bröer, S. (2000) Swelling-induced taurine release without chloride channel activity in *Xenopus laevis* oocytes expressing anion channels and transporters. *Biochim. Biophys. Acta* **1467**, 91–100
- 45 Guile, S. D., Bantick, J. R., Cooper, M. E., Donald, D. K., Eyssade, C., Ingall, A. H., Lewis, R. J., Martin, B. P., Mohammed, R. T., Potter, T. J. et al. (2007) Optimization of monocarboxylate transporter 1 blockers through analysis and modulation of atropisomer interconversion properties. *J. Med. Chem.* **50**, 254–263
- 46 Helgerson, A. L. and Carruthers, A. (1989) Analysis of protein-mediated 3-O-methylglucose transport in rat erythrocytes: rejection of the alternating conformation carrier model for sugar transport. *Biochemistry* **28**, 4580–4594
- 47 Carruthers, A. (1990) Facilitated diffusion of glucose. *Physiol. Rev.* **70**, 1135–1176
- 48 Nishimura, H., Pallardo, F., Seidner, G., Vannucci, S., Simpson, I. and Birnbaum, M. (1993) Kinetics of GLUT1 and GLUT4 glucose transporters expressed in *Xenopus* oocytes. *J. Biol. Chem.* **268**, 8514–8520
- 49 Rae, C., Nasrallah, F. A. and Broer, S. (2009) Metabolic effects of blocking lactate transport in brain cortical tissue slices using an inhibitor specific to MCT1 and MCT2. *Neurochem. Res.* **34**, 1783–1791
- 50 Kim, C. M., Goldstein, J. L. and Brown, M. S. (1992) cDNA cloning of MEV, a mutant protein that facilitates cellular uptake of mevalonate, and identification of a point mutation responsible for its gain in function. *J. Biol. Chem.* **267**, 23113–23121

SUPPLEMENTARY ONLINE DATA

AR-C155858 is a potent inhibitor of monocarboxylate transporters MCT1 and MCT2 that binds to an intracellular site involving transmembrane helices 7–10

Matthew J. OVENS*, Andrew J. DAVIES*, Marieangela C. WILSON*, Clare M. MURRAY† and Andrew P. HALESTRAP*¹

*Department of Biochemistry, School of Medical Sciences, University of Bristol, University Walk, Bristol BS8 1TD, U.K., and †Bioscience Department, AstraZeneca R&D Charnwood, Bakewell Road, Loughborough, Leicestershire LE11 5RH, U.K.

Table S1 Primers used in PCR generation of chimaeric MCTs

MCT form	MCT fragment	Left-hand primer	Right-hand primer
MCT1/4	MCT1 (TM1–6)	TCTTGGAAATTCATCGACACCT	GGACAAGTCCAGGAATTTATTAAC
	MCT4 (TM7–12)	CTGGACTTGTCCGTCTCCGAGAC	GGACCTCTCCCTGCTCCCTGC
MCT4/1	MCT4 (TM1–6)	CCAAGGTGAAACAGCCCTCCTGG	GGACAAGTCCAGCAGGGCGGG
	MCT1 (TM7–12)	CTGGACTTGTCCCTGTTTAC	ACACAAATGTCCTGTCT
MCT1/4TM11	MCT1 (N-terminus to TM10)	TCTTGGAAATTCATCGACACCT	CCCACAGCACTGGAGAAC
	MCT4 (TM11/12 and C-terminus)	CCCAGAGGTTCTCCAGTGC	GGACCTCTCCCTGCTCCCTGC
MCT4/1TM11	MCT4 (N-terminus to TM10)	CCAAGGTGAAACAGCCCTCCTGG	CCCACAGCACTGGAGAAC
	MCT1 (TM11/12 and C-terminus)	CCCAGAGGTTCTCCAGTGC	ACACAAATGTCCTGTCT
MCT1trnc	MCT1 (N-terminus to TM12 end)	TCTTGGAAATTCATCGACACCT	AAGTCGATAATTGATGCC
MCT1/4c	MCT1 (TMs)	TCTTGGAAATTCATCGACACCT	GCAGCACAAGGGAAGAGGTAGAGCCT
	MCT4 (C-terminus)	AGGCCTCTACCTTCCCTTGCTGCTGC	GGACCTCTCCCTGCTCCCTGC
	Site-directed mutagenesis	GGCCTCTACCTTCCCTTGCTGCTGCTGC (sense strand primer)	CAGCAGCAGCACAAGGAAGAGGTAGAGGCC (antisense strand primer)
MCT4/1c	MCT4 (TMs)	CCAAGGTGAAACAGCCCTCCTGG	CCCATAACAATGAGGAGGTGAGCACCT
	MCT1 (C-terminus)	AGGTGCTCACCTCCTATTGGTATGGG	ACACAAATGTCCTGTCT
	Site-directed mutagenesis	CCTCCTCATTGGATTGGGCATCAATTATCG (sense strand primer)	CGATAATTGATGCCAATACCAATGAGGAGG (antisense strand primer)

Table S2 crRNA injection quantities and [¹⁴C]-substrate uptake times used for *Xenopus* oocyte transport studies

N/A, not applicable.

MCT form	AR-C155858 studies		Kinetic studies	
	crRNA injected (ng)	[¹⁴ C]-substrate uptake time for assay (min)	crRNA injected (ng)	[¹⁴ C]-substrate uptake time for assay (min)
MCT1	20	2.5	5 (for L-lactate) 2 (for pyruvate)	5 5
MCT4	20	2.5	5 (for L-lactate) 20 (for pyruvate)	5 10 (for 0.2, 0.5, 1, 2 and 5 mM)
MCT1/4	20	20	20 (for L-lactate) 10 (for pyruvate) 10 (for 20, 50 and 75 mM)	20 (for 0.2, 0.5, 1, 2 and 5 mM) 5 (for 20, 50 and 75 mM) 5 (for 0.2, 0.5, 1, 2 and 5 mM)
MCT4/1	20	20	N/A	N/A

Received 30 September 2009/3 November 2009; accepted 20 November 2009
Published as BJ Immediate Publication 20 November 2009, doi:10.1042/BJ20091515

¹ To whom correspondence should be addressed (email a.halestrap@bristol.ac.uk).